Eur Biophys J 21, 21–28 (1992)

European Biophysics Journal

Size distribution of submicron particles by dynamic light scattering measurements: analyses considering normalization errors*

H. Ruf, E. Grell, and E. H. K. Stelzer**

Max-Planck-Institut für Biophysik, Kennedy-Allee 70, W-6000 Frankfurt 70, Federal Republic of Germany

Received October 18, 1991/Accepted in revised form November 29, 1991

Abstract. Errors in the experimental baseline used to normalize dynamic light scattering data can seriously affect the size distribution resulting from the data analysis. A revised method, which incorporates the characteristics of this error into the size distribution algorithm CONTIN (Ruf 1989), is tested with experimental data of high statistical accuracy obtained from a sample of phospholipid vesicles. It is shown that the various commonly used ways of accumulating and normalizing dynamic light scattering data are associated with rather different normalization errors. As a consequence a variety of solutions differing in modality, as well as in width, are obtained on carrying out data analysis in the common way. It is demonstrated that a single monomodal solution is retrieved from all these data sets when the new method is applied, which in addition provides the corresponding baseline errors quantitatively. Furthermore, stable solutions are obtainable with data of lower statistical accuracy which results from measurements of shorter duration. The use of an additional parameter in data inversion reduces the occurrence of spurious peaks. This stabilizing effect is accompanied by larger uncertainties in the width of the size distribution. It is demonstrated that these uncertainties are reduced by nearly a factor of two on using the normalization error function instead of the 'dust term' option for the analysis of noisy data sets.

Key words: Dynamic light scattering – Normalization errors – Lipid vesicles – Size distribution

Introduction

The method of dynamic light scattering (DLS) is widely applied to determine diffusion coefficients of suspended particles undergoing Brownian motion in liquids. With spherical particles the hydrodynamic radii can be calculated from the Stokes-Einstein relation, $D = kT/(6\pi\eta r)$, where D is the diffusion constant, k Boltzmann's constant, T the absolute temperature, r the particle radius, and η the viscosity of the medium. In the case of polydisperse samples the distribution function, $S(\Gamma)$, is obtained from the inversion of

$$|g^{(1)}(\tau)| = \int_0^\infty S(\Gamma)\, e^{-\Gamma\tau}\, d\Gamma, \tag{1}$$

where $|g^{(1)}(\tau)|$ is the magnitude of the normalized first-order or field autocorrelation function, τ is the delay time, and $\Gamma = q^2 D$ the characteristic decay constant for particles of a given diffusion constant. $q = (4\pi n/\lambda)\sin(\Theta/2)$ denotes the scattering vector, with n being the refractive index of the medium, λ the wavelength of the incident light in vacuo, and Θ the scattering angle (the fundamentals of the method and evaluation techniques can be found in reviews by Pusey and Vaughan (1975) and Stock and Ray (1985); a review of its special application to unilamellar lipid vesicles has been given elsewhere (Ruf et al. (1989)). $S(\Gamma)\,d\Gamma$ represents the fraction of light scattered by particles of diffusion constant D in the direction of Θ. This is the product of the number of particles of this size, the polarizability and the scattering form factor. By including varying parts of this product into the kernel of (1), and replacing D by means of the Stokes-Einstein relation, one can obtain, from the inversions, number-, mass-, squared mass- or intensity distributions in terms of the particle radius. Estimating $S(\Gamma)$ from the experimental data of the first-order autocorrelation function is an ill-posed problem in the sense that even small errors may seriously influence the results from the inversion of (1) (Phillips 1962). The determination of reliable size distributions from DLS experiments thus requires data of extremely high accuracy (Pike et al. 1983), as has been demonstrated for various particle suspensions, including bimodal size distributions of calibrated polystyrene latex beads (Morrison et al. 1985; Weiner and Tscharnuter 1987) and phospholipid vesicles (Hallett et al. 1991).

* Dedicated to Manfred Eigen on the occasion of his 65th birthday

***Present address:* EMBL, W-6900 Heidelberg, Federal Republic of Germany

Offprint requests to: H. Ruf

When the direct intensity fluctuation method with photon counting is applied, the normalized photocount autocorrelation function, Y_k, is calculated from the signal for a set of discrete delay times τ_k. The values y_k of the corresponding normalized first-order autocorrelation function needed for the common size distribution algorithms are then obtained from Siegert's relation, $y_k = (Y_k - 1)^{1/2}$ (Siegert 1943). Owing to the statistical nature of the scattered signal and of photon detection, experimental data from measurements of finite duration are noisy. Normalization of the data by its experimental baseline $\hat{B}$, which usually deviates from its expectation value B by a small, unknown amount $\Delta B = (\hat{B} - B)$, introduces additional errors (Jakeman et al. 1971). Combining the statistical deviations in E_k, and taking the systematic errors from normalization into account, the experimental values of the normalized photocount autocorrelation function can be written as

$$Y_k = \left(1 - \frac{\Delta B}{\hat{B}}\right) \frac{C(\tau_k)}{\bar{n}^2} + \frac{E_k}{\hat{B}}, \tag{2}$$

where $C(\tau_k)/\bar{n}^2$ are the corresponding expectation values with $\bar{n}$ being the expectation value of the average number of counts per sampling time interval. Correspondingly, the values of the first-order autocorrelation function are

$$y_k = \left[\left(1 - \frac{\Delta B}{\hat{B}}\right) f(A) |g^{(1)}(\tau_k)|^2 - \frac{\Delta B}{\hat{B}} + \frac{E_k}{\hat{B}}\right]^{1/2}, \tag{3}$$

where $f(A)$ is a spatial coherence factor depending on the number of coherence areas viewed and on the sample time (Jakeman 1974). Noise in the data of the photocount autocorrelation function can be reduced, for example, by increasing the number of samples, that is by increasing the duration of measurements, which also holds for the statistical part of the error in the experimental baseline. Those parts of the baseline errors arising from other sources, such as the drift in the mean scattering intensity during the time of measurement might, however, become especially serious in low noise data accumulated from measurements of long duration. The fact that an error in the baseline value changes only the amplitude but not the decay characteristics of a normalized photocount autocorrelation function (Hughes et al. 1973) suggested that this type of error wouldn't be a very serious one. Nevertheless, the importance of the accuracy of the experimental baseline for obtaining useful results has been pointed out repeatedly (eg. Oliver 1981; Chu 1983). Using a single exponential decaying function, which simulates the photocount autocorrelation function of a monodisperse sample of submicron particles, Weiner and Tscharnuter (1987) demonstrated with the cumulant method (Koppel 1972) that even small errors will have drastic effects, particularly on the polydispersity parameter. They concluded that the baseline must be correctly established within at least 0.1%, or surprisingly large errors occur in any parameter which describes the width of the distribution. Recently, it has been shown that these drastic effects are a consequence of the square root extraction involved in Siegert's relation (Ruf 1989). This transforms the error such that it also modifies the decay characteristics of the corresponding first-order autocorrelation function. Even worse, the normalization error increases exponentially as the expectation value of the autocorrelation function decays. Because the commonly used size distribution algorithms do not take components with positive exponents into account, even small baseline errors will severely distort the size distributions resulting from data inversions, as has been demonstrated in the same paper with computer simulated data of a given monomodal size distribution. The analyses of these data were carried out with the size distribution algorithm CONTIN (Provencher et al. 1978, Provencher 1979, 1982a,b) yielding in the case of $\pm 0.25\%$ baseline errors either much too narrow size distributions or incorrectly bimodal ones.

To reduce errors arising from drifts of the mean scattering intensity, it has been suggested that one should perform a series of measurements of short duration instead of carrying out a single long time measurement, and then analyse the averages of these batches of individually normalized data sets (Jakeman et al. 1971). Experimentally, the problem of improving the accuracy of the baseline value was tackled by designing new correlators that allow one to measure the baseline over an extended range of delay times, and by using improved normalization schemes (Schätzel et al. 1988). An alternative approach, which improves the analysis of data from most of the currently used instrumentation and which may supplement the new developments in correlator design, is to include the characteristics of normalization errors into the inversion algorithm. It has been shown (Ruf 1989) that normalization errors in the data of first-order autocorrelation functions can be described approximately by

$$F(\tau_k) = -\frac{1}{2}\left[\frac{1}{f^{1/2}(A)|g^{(1)}(\tau_k)|} + f^{1/2}(A)|g^{(1)}(\tau_k)|\right]\frac{\Delta B}{\hat{B}} \tag{4}$$

or

$$\hat{F}(\tau_k) = -\frac{1}{2}\left[\frac{1}{y_k} + y_k\right]\frac{\Delta B}{\hat{B}}. \tag{5}$$

Equations (4) and (5) represent the linear terms in the relative baseline error $\Delta B/\hat{B}$ of the series expansion of (3). Expansion at the expectation values, $f^{1/2}(A)|g^{(1)}(\tau_k)|$, results in (4), while expanding it at the experimental values, y_k, yields (5). These two linear normalization error functions have been incorporated into Provencher's size distribution algorithm CONTIN, and their ability to reliably retrieve size distributions from erroneous data has been demonstrated with simulated autocorrelation functions (Ruf 1989).

The purpose of this paper is to investigate normalization errors in experimental data with this new method. The DLS measurements were carried out on a sample of phospholipid vesicles, submicron particles employed in many biophysical and biological studies. Unlike those used before (Stelzer et al. 1983), the vesicles used for these studies had greater internal volumes. They had an average diameter of about 200 nm and were prepared by dialysis according to Mimms et al. (1981), who showed that unilamellar vesicles of rather homogeneous size are obtained by this technique. It will be demonstrated here that

various commonly used sampling and normalization schemes in DLS measurements are associated with rather different normalization errors that cause very different size distributions to be obtained when carrying out data analyses in the common way. As is shown, these differences will disappear in the case of low noise data and will be small for data of higher noise content when the inversions are carried out by including the characteristics of normalization errors. We compare here the results obtained from data accumulated in a measurement of long duration with those obtained by averaging over a corresponding large batch of measurements of short duration, and the effects of two different kinds of normalization.

Materials and methods

Materials and preparations

Unilamellar lipid vesicles made from egg yolk phosphatidylcholine (PC) were prepared in 65 mM NaCl, 20 mM PIPES-NaOH buffer, pH 7.2 by a dialysis similar to that used by Mimms et al. (1981) as described before (Kojro et al. 1989), using a molar detergent (*n*-octyl-β-D-glucopyranoside) to lipid ratio of 10:1. All chemicals were of analytical grade and were obtained from Merck or Fluka. Water was purified by Milli-Q columns (Millipore, Bedford, MA). The vesicle dispersion, characterized by a phosphorus content of 0.2 mM, was filtered through a 0.4 μm Nuclepore polycarbonate filter into the cylindrical light scattering cuvette (⌀10 mm).

Data collection and analysis

The scattering experiments were carried out with a light scattering goniometer from ALV (Langen, Germany). The light source was a Spectra Physics, Model 124 B, 15 mW, linearly polarized HeNe laser. The index matching fluid surrounding the sample cell was toluene (Merck, optical grade). Details on focusing optics, sample cell assembly, vibration isolated table, and constant temperature maintenance in the sample cell and the surrounding liquid have been described elsewhere (Georgalis et al. 1987).

The signal from the detection unit (Malvern Model RF 313) was sent to a BI 2020 correlator from Brookhaven Instruments Corp. The correlator has 136 channels followed by 8 baseline channels starting at 1024 sample times. The correlator was externally controlled by a FORTRAN program running on a Hewlett Packard HP 1000 minicomputer. The series of short-time measurements were carried out as follows. The control program set the sample time and the total number of samples in the correlator before it started the first run. It initiated data transfer and storage upon completion and repeated these three operations a preset number of times. The autocorrelation function of each short-time run was visually inspected and analysed by the cumulant method to check the data for experimental artifacts. Data analysis was carried out on the HP 1000 computer. The mass-weighted size distributions in terms of the vesicle radius were obtained with the modified version of the program CONTIN that allows one to take baseline errors into account. With the recent version, the procedure described before (Ruf 1989) is considerably simplified. In the preliminary, unweighted analysis the coefficients of the normalization error function are calculated as before the input data according to (5), but in the final weighted analysis these are now calculated from the chosen solution of the preliminary unweighted analysis according to (4).

The range of delay times applied for measuring the photocount autocorrelation function spanned roughly two characteristic mean decay times. For relative baseline errors of about 10^{-3}, typical of the experiments presented here, the true normalization errors in data of this decay range are well approximated by both error functions, (4) and (5). The maximum deviation from the true normalization error at the right-hand point of the decay curve is only 0.6%. The numerical integration in (1) was performed using Simpson's rule with 31 linearly spaced grid points. The size limits selected for the first data inversion were derived from the delay time of the first correlator channel and from three times the mean decay time. This range was then adjusted to narrower size limits, such that only a few grid points near either integration limit were associated with zero amplitude of the size distribution. The size distribution was additionally forced to be zero at two extra points outside either integration limit by specifying the corresponding control parameters of the program. The size range found to be optimal for the inversion of the batch data normalized by the baseline value determined from the total number of counts was used throughout the analysis. The scattering form factor (Pecora and Aragon 1974) and the volume of spherical shells were included into the kernel of (1), to obtain from the inversion the distribution of particulate mass density. A thickness of 4.5 nm was taken for the vesicle shell. The distributions shown here were normalized so that the integral of all values in the radius is unity. The range of the damping parameter (α-grid) was adjusted to give solutions selected by the *F*-test with Prob1(α)-to-reject values between 0.48 and 0.52 (Provencher 1982 a, c). The dynamic light scattering experiments were carried out at 20 °C, and at an angle of 90 deg. The viscosity and refractive index of water were used for the data analysis.

Results and discussion

To demonstrate the effects of normalization errors occurring for reasons unconnected with the statistical properties of the signal requires low noise data. Unfortunately, unlike the case of monodisperse particles (Jakeman et al. 1971; Degiorgio and Lastovka 1971; Saleh and Cardoso 1973; Schätzel 1990) no corresponding quantitative relation exists for polydisperse systems, from which the minimal duration of a DLS measurement can be calculated for a desired noise level. Measuring times of many hours have been reported to be appropriate for the determination of size distributions of some more complex particle systems (Morrison et al. 1985). Instead of merely taking these numbers, the time actually required for resolving

the size distribution of our vesicle system within a few percent of error was estimated from results obtained with simulated noisy autocorrelation functions. This alternative was chosen because the minimal measurement duration depends on both the modality of a distribution and the widths of the peaks, as well as on features of the experimental set-up such as detector aperture, power of the laser light source and multi-bit resolution of the correlator. For our particular system a considerably shorter measuring time of about 4 h was found to be sufficient. The simulations were carried out as follows. A second-order autocorrelation function was simulated for a Schulz distribution of hollow spheres (see Aragon and Pecora 1976) of mass-weighted mean radius $r_m = 104.6$ nm and width $s_m = 23$ nm, being related to a z-parameter of 17 (the distribution width is characterized by the mean deviation $s_m = [M_2/M_0 - (M_1/M_0)^2]^{1/2}$ with M_0, M_1, and M_2 being the moments of the distribution function of order 0, 1 and 2 with respect to the vesicle radius). These values were estimated from preliminary results of DLS measurements with vesicles prepared according to the procedure described in the experimental section. Poisson type noise was added according to (9) given in the article of Provencher (1979) using a random number generator. The sample time interval was 10 μs, and a total number of 1.5×10^9 samples were taken, which corresponds to a total measurement duration of 4 h and 10 min. At a mean rate of 0.5 counts per sample time interval, the baseline of the N-fold photocount autocorrelation function becomes 3.75×10^8. Five different sets of 136 data points each, with noise contents ranging from 3.8×10^{-7} to 4.7×10^{-7} as characterized by the sum of the squared deviations, were analysed with the modified version of CONTIN. The inversions were performed with and without a normalization error function. The results are summarized in Table 1, and a typical size distribution of each series is depicted in Fig. 1. The solutions selected by the program from inversions with the error function are slightly broader than those obtained from inversions without additional parameters. Such behaviour is also observed when a constant background is taken into account instead. Generally, the use of an additional parameter has a broadening effect on the solution selected by the program. However, this is valid only in a statistical sense, as in a few cases narrower size distributions will also be obtained. Within each series the mean radii differ by less than 0.3% and the agreement of the widths is better than 1%, indicating that this noise level is indeed sufficiently low for obtaining reliable results in the case of this monomodal size distribution. It should be mentioned that noise simulating only the statistics of photon detection does not completely reflect the experimental situation. Noise arising from the statistical nature of the intensity fluctuations, which is sometimes called 'signal noise', dominates at average rates of about 0.5 counts per sample time (Jakeman et al. 1971). This type of noise is correlated in adjacent data points (Saleh and Cardoso 1973), and therefore will have stronger effects on the results than purely random noise. Nevertheless, the time requirements concluded from these simulations are appropriate to determine the size distribution of vesicles within a few percent of error.

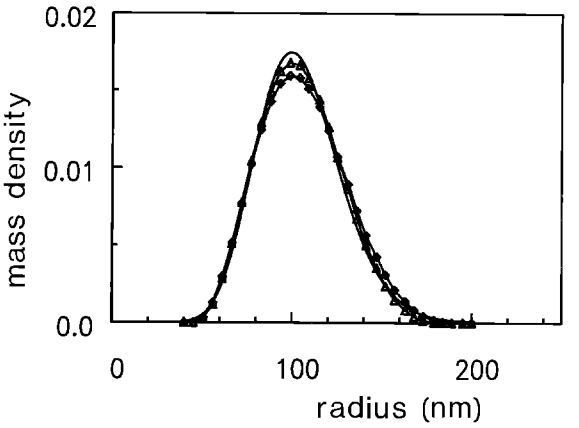

Fig. 1. Mass density distributions obtained from noisy DLS data simulating the light scattered by a Schulz-distribution of unilamellar vesicles (—) plotted versus the hydrodynamic radius. Data inversions were performed without fitting additional parameters (△) and with the normalization error function (◇)

Table 1. Averaged mass weighted mean radii and widths obtained from the analysis of 5 sets of simulated noisy data with and without the normalization error function

	$\bar{r}_m$ [nm]	$\overline{s_m/r_m}$	$\overline{\Delta B/\bar{B}}$, 10^{-4}
	104.1 (0.09)[a]	0.215 (0.4)	–
	105.7 (0.08)	0.226 (0.5)	4.3 (7)
Original distribution	104.6	0.222	

[a] Numbers in parenthesis are percent root-mean-square deviations

For the DLS experiments with unilamellar phospholipid vesicles, 25 runs of 10 min duration were carried out (the mean count rate drift was 2% per hour). Normalizing each run by its experimental baseline and subsequently averaging all 25 measurements yielded the batch data set. Accumulating the raw data of the individual runs and normalizing this data set with the sum of the corresponding baseline values gave the so called long data set, just as if the experiment were carried out as a measurement of long duration. These two different ways of accumulating the raw data allows comparison of the two sampling modes directly on the same set of experimental data, without having the imponderables of two separate measurements. Normalization was performed as 'self' and 'far-point' employing the notation of Oliver (1981). For 'self' normalization the content of the correlator channels, $\hat{C}(\tau_k)$, is divided by the value of the baseline, B_s, calculated from the total number of photon counts

$$Y_k = \hat{C}(\tau_k)/B_s, \tag{6}$$

whereas with 'far-point' normalization

$$Y_k = 1 + (\hat{C}(\tau_k) - B_f)/B_s, \tag{7}$$

the average content of some delay or baseline channels, B_f, is used in addition (we use here B_s instead of the long term average of the baseline involved in the original definition). For comparison, the batch data were additionally normalized according to (6) but with B_f instead of B_s.

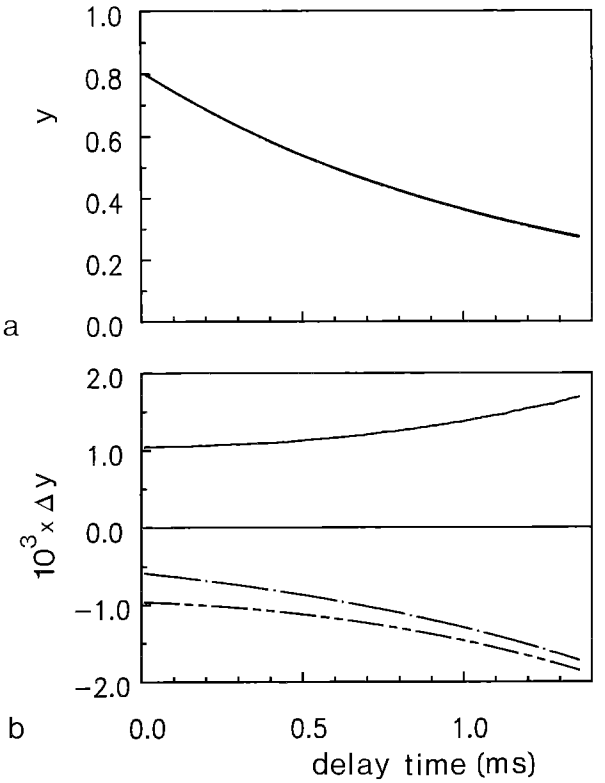

Fig. 2. a Experimental first-order autocorrelation functions ($N = 1.5 \times 10^9$, $\delta t = 10$ µs) of long data set, 'self'- and 'far-point' normalized batch data plotted versus delay time. **b** Difference curves of the long data set (—), 'far-point' normalized batch data (– · –), and batch data normalized with B_f according to 5 (– · · –) with regard to the 'self' normalized batch data. All three difference curves exhibit the typical features of normalization errors

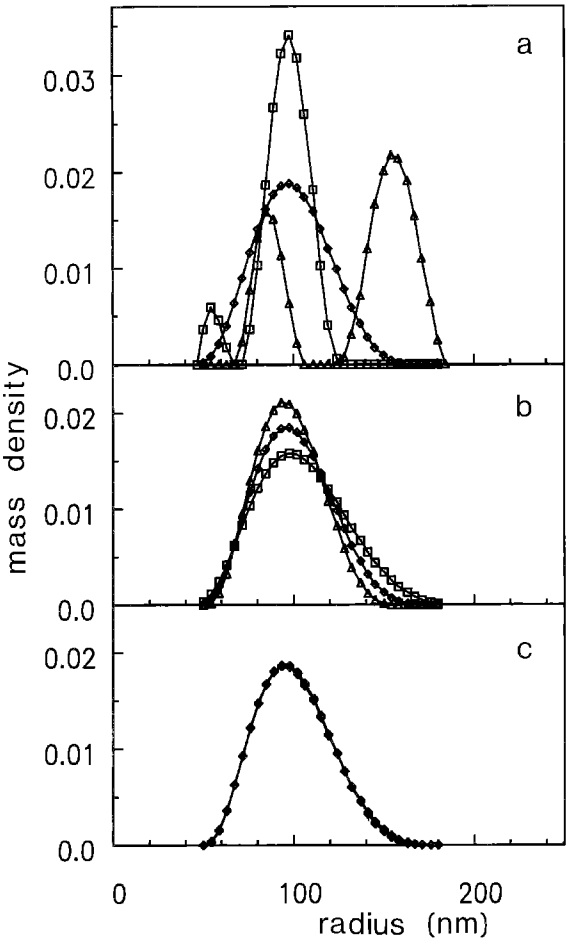

Fig. 3 a–c. Mass density distribution resulting from the analysis of DLS measurements on a sample of unilamellar phospholipid vesicles plotted versus the hydrodynamic radius. Size distributions obtained from the long data set (△), 'far-point'-(□) and 'self' normalized batch data (○) are plotted versus the hydrodynamic radius. Data inversions are performed: **a** without additional parameters; **b** with a constant background; **c** with a baseline error (since all three solutions are practically identical, only one symbol is used here)

The first-order autocorrelation functions of these different data sets, and their differences with regard to the 'self' normalized batch data are shown in Fig. 2. All three difference curves exhibit the typical exponential increase of normalization errors with increasing delay time, which indicates that the various sampling and normalizing schemes in autocorrelation functions are associated with different normalization errors. The effects of these errors on the results of data inversion are depicted in Fig. 3 (the size distributions returned from the additional data set were almost identical to those obtained from the 'far-point' normalized data, and therefore have been omitted). The inversions without additional parameters yield rather different solutions (Fig. 3 a). While a monomodal distribution is obtained from the 'self' normalized batch data, the other two data sets yield different bimodal solutions. Taking a 'dust term' into account reduces this ambiguity and yields only monomodal size distributions but still with a considerable spread in width (Fig. 3 b). Yet, when the normalization error function is used practically a single solution is obtained from all three data sets (Fig. 3 c). The values of relative baseline errors (Table 2) indicate that the 'self' normalized batch data set is the most accurate one, as expected. There, the relative baseline error is only about 10^{-4}. Consistently, the distributions obtained from the analysis with the three different options are essentially the same. The baseline errors of the two other data sets are about one order of magnitude larger and are different in sign. A negative sign means that the experimental value of the baseline is smaller than its expectation value, which is the case for the long data set. The baseline value calculated from the eight delay channels, on the other hand, is larger than its expectation value. This result is consistent with slowly decaying contributions due to minute amounts of dust, which are nearly always present in a dispersion.

The use of a 'dust term' as additional parameter also provides monomodal size distributions from all data sets, but with a considerable spread in mean size and width (Fig. 3 b). Moreover, the values obtained for the background are far too large, as has been checked by measuring the autocorrelation function at longer delay times. In the case of the 'far-point' normalized batch data the sign of the background value is negative which would be physically unreal. Yet when data of a second-order autocorrelation function are normalized by baseline values that are too large the baseline of the corresponding first-order autocorrelation function, which ideally is zero, becomes

Table 2. Parameters of the size distributions of lipid vesicles obtained from the three different data sets applying various options upon data inversion

Data inversion	Without additional parameters		With a constant background			With the normalization error function		
	r_m [nm]	s_m/r_m	r_m [nm]	s_m/r_m	B_c, 10^{-3}	r_m [nm]	s_m/r_m	$\Delta B/\hat{B}$, 10^{-4}
'Self' normalized long data set	86.4 155.5	0.083 0.071	97.4	0.179	5.9	100.3	0.203	−9.4
'Self' normalized batch data	99.7	0.198	100.1	0.202	−0.19	100.1	0.201	−0.97
'Far point' normalized batch data	56.3 97.7	0.066 0.102	104.4	0.229	−7.1	100.4	0.204	8.5

Table 3. Mass-weighted mean radii and widths of size distributions of lipid vesicles obtained from data batches of different size

Batch size	No.	$\bar{r}_m$ [nm]	$\overline{s_m/r_m}$	$\overline{\Delta B/\hat{B}}$, 10^{-4}
25	1	100.1	0.201	−0.97
18	1	100.4	0.204	−0.05
	2	98.4	0.185	−2.9
	3	100.7	0.208	2.4
	av[a]	99.8 (1.3)[b]	0.199 (6.2)	
12	1	102.4	0.220	4.7
	2	98.0	0.182	−2.6
	3	101.4	0.215	3.1
	4	98.4	0.183	−5.0
	av	101.1 (2.2)	0.200 (10)	

[a] Averages over the corresponding number of data sets
[b] Numbers in parentheses are percent root-mean-square deviations

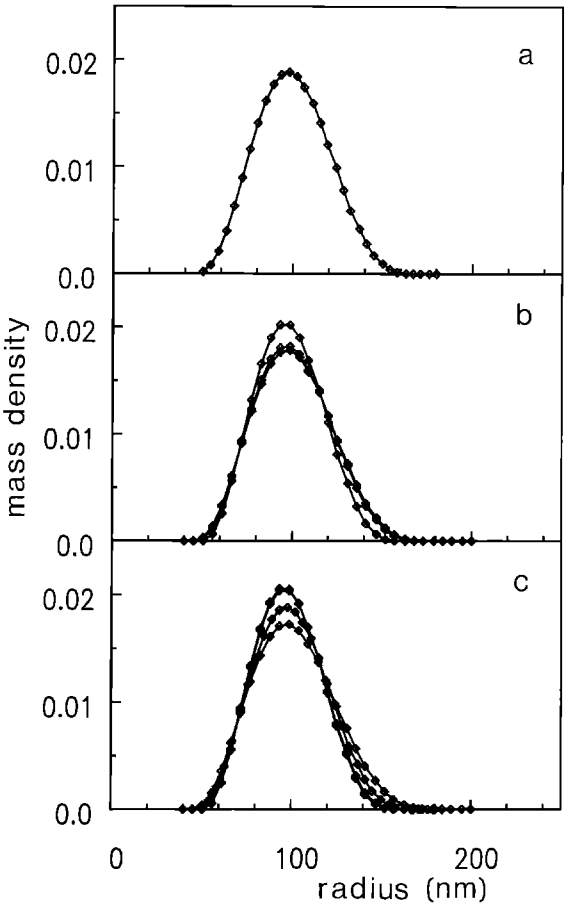

Fig. 4 a–c. Phospholipid vesicles: mass density distributions obtained from inversions with the baseline error function from batches of different size plotted versus the hydrodynamic radius: **a** 1 batch of 25 short-time runs; **b** 3 batches of 18 short-time runs; **c** 4 batches of 12 short-time runs. Panels b and c illustrate the variations in resulting inversions in dependence of measurement duration

negative, and consequently a negative value is returned from the analysis with the 'dust term' option (Ruf 1989). Thus, the finding of a negative background may in turn be indicative of a positive baseline error.

The results of our analyses show that the major differences in the three data sets are due to normalization errors, and that a single solution is obtained with the new method. The high stability of this solution with regard to the different sampling and normalization schemes suggests that it represents the vesicle size distribution of our dispersion. The remaining uncertainties due to the noise still present in the experimental data were estimated to be about 1% for the mean size and about 3% for the width. These numbers were extrapolated from the results obtained with various shorter batches of 12 and 18 'self' normalized short-time runs constructed out of the total of 25 measurements. The higher noise content in these data sets causes a larger spread in mean size and widths of the solutions. The dependence of this spread on the level of noise allows an estimate of the accuracy of the solution obtained from the complete batch. The results of the analyses of smaller batches are shown in Fig. 4, and the characteristic parameters of the distributions are summarized in Table 3. Accordingly, the accuracies of the mean radius determined from 2 h and 3 h measurements are about 3% and 2%, respectively, and 10% and 6% for the width. Actually, these accuracies might not be as high, because it cannot be excluded that some of the vesicles are multilamellar. However, comparison with the size distribution reported by Mimms et al. (1981), as determined from electron microscopy, shows a very good agreement. The peaks of the two distributions fit nicely. From the electron micrographs a greater fraction of larger vesicles was determined than from our DLS data, and correspondingly a larger average diameter of 240 nm ± 60 nm was reported. These differences may reflect slight differences in the preparations, but may be also due in part to effects of the

staining procedure and particularly to the limited statistics in the evaluation of the electron micrographs.

The analysis of data sets with higher noise content, formed from smaller batches of 'self' normalized data, without additional parameters, demonstrates the ill-posed nature of the inversion of (1). In nearly half of the cases one obtains bimodal solutions with mean radii of 95 nm and 170 nm. The use of either a 'dust term' or a baseline error as additional parameters stabilizes the solution again, but at the expense of mostly too broad size distributions. This broadening effect is directly related to the noise content, as has also been found before (Flamberg and Pecora 1984; Vaidya et al. 1987). With the 'dust term' option the mean radius of our vesicle dispersion is determined from 2 h and 3 h measurements with accuracies of about $\pm 5\%$ and $\pm 2.5\%$, and the width with accuracies of about $\pm 19\%$ and $\pm 10\%$, respectively. Comparison with the corresponding values in Table 3 shows that an improvement of the accuracies of the distribution parameters by roughly a factor of two is achieved if the baseline error option is used. From our experience of the analysis of experimental and simulated data with the program CONTIN we inferred that there is an interrelation between the noise content, the solution selected by the program according to the F-test, and the magnitude of the additional parameter, which we were not able to quantify. We found empirically that in data of higher noise content the use of an additional parameter generally reduces the occurrence of spurious peaks but at the expense of mostly too broad size distributions and too large values of the additional parameter (as concluded from simulated data). Thereby, the normalization error function provides solutions with considerably smaller uncertainties and less unrealistic values of the additional parameter than the 'dust term' option. This special property of the normalization error function in the case of noisy data, however, is not fully understood yet.

The version of CONTIN we used for data analysis employed the Poisson statistics of photon detection for calculating the weights of data. In the case of noisy data resulting from measurements of shorter duration an improvement is to be expected when sampling is carried out at multiple sample times and the statistics of the intensity fluctuations of 'diffusional' noise are included in weighting the data (Schätzel 1990; Peters 1991). The experimental duration of about 4 h used here is related to the characteristics of this particular size distribution, and to the limitations of the linear correlator available for this study. In general, broad distributions are more easily obtained than narrow or more complex ones (Schätzel 1987). Recently, attempts to quantify this relationship for monomodal size distributions have been made (Kojro 1990). The numbers given there, however, underestimate the actual temporal requirements for the particular vesicle system investigated here by roughly two orders of magnitude. In this article it has been claimed, in addition, that normalization errors would not exist because of a 'self compensation phenomenon'. This statement is inconsistent with our experimental data. A general relationship that allows derivation of the accuracies with which size distributions can be determined directly from given noise levels would be desirable. The analysis of simulated data, which is applied here, is a rather tedious alternative. A more promising approach is to pursue the stabilization of the solution of the inversion during the measurement, where it should be kept in mind that the improvement is hyperbolic in time rather than linear. This now starts to become available with modern fast computing techniques. The use of the normalization error function in data analysis supplements this approach and speeds up the search for stable and reliable size distributions.

Conclusions

For relative baseline errors ranging from 10^{-4} to about 2×10^{-3} it is generally sufficient to carry out only one inversion with the modified program. With larger baseline errors, rarely observed in the case of low noise data measured under stable conditions, an iterative procedure is suggested. Because the normalization errors are no longer completely described by the linear approximations in all data, the inversions mostly yield overestimates of the actual baseline error. The data then have to be renormalized by a fraction of the overestimated error value and inverted again. This procedure has to be repeated until a stable solution is obtained. Baseline errors smaller than 10^{-4} do not actually require the use of the normalization error function. However, it is good practice when using this function to find out whether normalization errors are present in the data and to eventually perform a second inversion without additional parameters. The use of the normalization error function is also advantageous with data of higher noise content arising from measurements of shorter duration, when higher inaccuracies of the distribution parameters are tolerable. The analysis with the error function was found to yield solutions with a minimal spread in width and modality. There are limits in shortening the total measurements duration, which can be fairly high if narrow or more complex continuous size distributions are to be determined. The shortest total duration of measurements, from which here only monomodal size distribution are returned, lies somewhere in between 1 and 2 h. This temporal limit is not an absolute one, of course. It is related, in addition, to features of our experimental set-up such as intensity of the laser light source, aperture of the detector, resolution of the correlator, and weighting of data in our analysis. Modern instrumentation and proper weighting schemes will lower this limit. Nevertheless, it provides reasonable clues to the temporal requirements for the determination of monomodal size distribution of this width.

Acknowledgement. The authors wish to thank Daniel Grell for preparation of the vesicles.

References

Aragon SR, Pecora R (1976) Theory of dynamic light scattering from polydisperse systems. J Chem Phys 64:2395–2404

Chu B (1983) Correlation function profile analysis in laser light scattering I. General review on methods of data analysis. In: Earnshaw JC, Steer MW (eds) The application of laser light

scattering to the study of biological motion, NATO Adv Sci Inst Series A, vol 59. Plenum Press, New York London, pp 53–76
Degiorgio V, Lastovka JB (1971) Intensity-correlation spectroscopy. Phys Rev A 4:2033–2050
Flamberg A, Pecora R (1984) Dynamic light scattering study of micelles in a high ionic strength solution. J Phys Chem 88:3026–3033
Georgalis Y, Ruf H, Grell E (1987) Photon-correlation-spectroscopy of membrane model systems. In: Burgen ASV, Roberts GCK, Anner BM (eds) Topics in molecular pharmacology, vol 4. Elsevier, Amsterdam, pp 1–20
Hallett FR, Watton J, Krygsman P (1991) Vesicle sizing – number distributions by dynamic light scattering. Biophys J 59:357–363
Hughes AJ, Jakeman E, Oliver CJ, Pike ER (1973) Photon-correlation spectroscopy: dependence of linewidth error on normalization, clip level, detector area, sample time and count rate. J Phys A: Math Nucl Gen 6:1327–1336
Jakeman E (1974) Photon correlation. In: Cummins HZ, Pike ER (eds) Photon correlation and light beating spectroscopy, NATO Adv Study Inst Series B, vol 3. Plenum Press, New York London, pp 75–149
Jakeman E, Pike ER, Swain S (1971) Statistical accuracy in the digital autocorrelation of photon counting fluctuations. J Phys A: Gen Phys 4:517–534
Kojro Z (1990) Influence of statistical errors on size distributions obtained from dynamic light scattering data. Experimental limitations in size distribution determination. J Phys A: Math Gen 23:1363–1383
Kojro Z, Lin SQ, Grell E, Ruf H (1989) Determination of internal volume and volume distribution of lipid vesicles from dynamic light scattering data. Biochim Biophys Acta 985:1–8
Koppel DE (1972) Analysis of macromolecular polydispersity in intensity correlation spectroscopy: the method of cumulants. J Chem Phys 57:4814–4820
Mimms LT, Zampighi G, Nozaki Y, Tanford C, Reynolds JA (1981) Phospholipid vesicle formation and transmembrane protein incorporation using octyl glucoside. Biochemistry 20:833–840
Morrison ID, Grabowski EF, Herb CA (1985) Improved techniques for particle size determination by quasi-elastic light scattering. Langmuir 1:496–501
Oliver J (1981) Recent development in photon correlation and spectrum analysis techniques: II. Information from photodetection spectroscopy. In: Chen SH, Chu B, Nossal R (eds) Scattering techniques applied to supramolecular and nonequilibrium systems, NATO Adv Sci Inst Series B, vol 73. Plenum Press, New York London, pp 121–160
Pecora R, Aragon SR (1974) Theory of light scattering from hollow spheres. Chem Phys Lipids 13:1–10
Peters R (1991) Noise on photon correlation functions and its effect on data reduction algorithms. In: Brown W (ed) Dynamic light scattering, the method and some application. Oxford University Press, Oxford (in press)
Phillips DL (1962) A technique for the numerical solution of certain integral equations of the first kind. J Ass Comput Mach 9:84–97
Pike ER, Watson D, McNeil Watson F (1983) Analysis of polydisperse scattering data II. In: Dahneke BE (ed) Measurement of suspended particles by quasi-elastic light scattering. Wiley, New York, pp 107–128
Provencher SW (1979) Inverse problems in polymer characterization: direct analysis of polydispersity with photon correlation spectroscopy. Makromol Chem 180:201–209
Provencher SW (1982a) A constrained regularization method for inverting data represented by linear algebraic or integral equations. Comput Phys Commun 27:213–227
Provencher SW (1982b) CONTIN: A general purpose constrained regularization programm for inverting noisy linear algebraic and integral equations. Comput Phys Commun 27:229–242
Provencher SW (1982c) CONTIN, Users Manual. EMBL technical report DA05. Heidelberg: European Molecular Biology Lab
Provencher SW, Hendrix J, De Maeyer L, Paulussen N (1978) Direct determination of molecular weight distributions of polystyrene in cyclohexane with photon correlation spectroscopy. J Chem Phys 69:4273–4276
Pusey PN, Vaughan JM (1975) Light scattering and intensity fluctuation spectroscopy. In: Davies M (ed) Dielectric and related molecular processes, vol 2. The Chemical Society, London, pp 48–105
Ruf H (1989) Effects of normalization errors on size distributions obtained from dynamic light scattering data. Biophys J 56:67–78
Ruf H, Georgalis Y, Grell E (1989) Dynamic light scattering to determine size distributions of vesicles. In: Fleischer S, Fleischer B (eds) Methods in enzymology, biomembranes part S, vol 172. Academic Press, San Diego, pp 364–390
Saleh BEA, Cardoso MF (1973) The effect of channel correlation on the accuracy of photon counting digital autocorrelators. J Phys A Math Nucl Gen 6:1897–1909
Schätzel K (1987) Correlation techniques in dynamic light scattering. Appl Phys B 42:193–213
Schätzel K (1990) Noise on photon correlation data: I. Autocorrelation functions. Quant Opt 2:287–305
Schätzel K, Drewel M, Stimac S (1988) Photon correlation measurements at large lag times: improving statistical accuracy. J Mod Opt 35:711–718
Siegert AJF (1943). MIT Rad Lab Rep No 465
Stelzer EHK, Ruf H, Grell E (1983) Analysis and resolution of polydisperse systems. In: Schulz-Dubois EO (ed) Photon correlation techniques, Springer Series in Optical Sciences, vol 6. Springer, Berlin Heidelberg New York, pp 329–334
Stock RS, Ray WH (1985) Interpretation of photon correlation spectroscopy data: A comparison of analysis methods. J Polym Sci Polym Phys 23:1393–1447
Vaidya RA, Mettille MJ, Hester RD (1987) A comparison of methods for determining macromolecular polydispersity from dynamic light scattering data. In: Provder T (ed) Particle size distribution, ACS Symposium Series, vol 332. American Chemical Society, Washington DC, pp 62–73
Weiner BB, Tscharnuter WW (1987) Uses and abuses of photon correlation spectroscopy. In: Provder T (ed) Particle size distribution, ACS Symposium Series, vol 332. American Chemical Society, Washington DC, pp 48–61